Nuclear Instruments and Methods in Physics Research B 365 (2015) 325–330

Contents lists available at ScienceDirect

Nuclear Instruments and Methods in Physics Research B

journal homepage: www.elsevier.com/locate/nimb

# Heavy and light ion irradiation damage effects in δ-phase $Sc_4Hf_3O_{12}$

J. Wen [a,b], Y.H. Li [a,*], M. Tang [b], J.A. Valdez [b], Y.Q. Wang [b], M.K. Patel [c], K.E. Sickafus [c]

[a] School of Nuclear Science and Technology, Lanzhou University, Lanzhou, Gansu 730000, China
[b] Materials Science and Technology Division, Los Alamos National Laboratory, Los Alamos, NM 87545, USA
[c] Department of Materials Science & Engineering, The University of Tennessee, Knoxville, TN 37996, USA

ARTICLE INFO

*Article history:*
Received 2 October 2014
Accepted 5 April 2015
Available online 16 April 2015

*Keywords:*
Irradiation damage effects
Phase transformation
TEM
GIXRD

ABSTRACT

Polycrystalline δ-phase $Sc_4Hf_3O_{12}$ was irradiated with light and heavy ions to study the radiation stability of this compound. In order to explore the ion species spectrum effect, the irradiations were performed with 400 keV $Ne^{2+}$ ions to fluences ranging from $1 \times 10^{14}$ to $1 \times 10^{15}$ ions/cm$^2$, 600 keV $Kr^{3+}$ ions to fluences ranging from $5 \times 10^{14}$ to $5 \times 10^{15}$ ions/cm$^2$, and 6 MeV $Xe^{26+}$ ions to fluences ranging from $2 \times 10^{13}$ to $1 \times 10^{15}$ ions/cm$^2$. Irradiated samples were characterized by various techniques including grazing incidence X-ray diffraction (GIXRD) and transmission electron microscopy (TEM). A complete phase transformation from ordered rhombohedral to disordered fluorite was observed by a fluence of $1 \times 10^{15}$ ions/cm$^2$ with 400 keV $Ne^{2+}$ ions, equivalent to a peak ballistic damage dose of ~0.33 displacements per atom (dpa). Meanwhile, the same transformation was also observed by 600 keV $Kr^{3+}$ ions at the same fluence of $1 \times 10^{15}$ ions/cm$^2$, which however corresponds to a peak ballistic damage dose of ~2.2 dpa. Only a partial O-D transformation was observed for 6 MeV $Xe^{26+}$ ions in the fluence range used. Experimental results indicated that the O-D transformation is observed under both electronic and nuclear stopping dominant irradiation regimes. It was also observed that light ions are more efficient than heavy ions in producing the retained defects that are presumably responsible for the O-D phase transformation. The O-D transformation mechanism is discussed in the context of anion oxygen Frenkel defects and cation antisite defects. We concluded that the irradiation induced O-D transformation is easier to occur in δ-phase compounds with partial order of cations than in that with fully disordered cation structures.


## 1. Introduction

With the expanded application of nuclear power all over the world in the past half-century, substantial quantities of nuclear waste, such as plutonium and minor actinides (Np, Am and Cm), have been generated from nuclear fuel cycles. A considerable amount of research has been done in an effort to search for radiation-tolerant materials that can be used as an inert matrix in nuclear fuels and as host materials for minor actinides in high-level radioactive waste [1–5]. Such waste form materials should have a high capacity for incorporating actinides, possess a high radiation resistance and excellent chemical stability. Crystalline oxides that possess the fluorite ($CaF_2$) structure or the derivatives of the fluorite structure have received considerable attention as candidate materials for nuclear-waste host. The compounds of interest in this investigation are oxygen-deficient fluorite structural derivatives $MO_{2-x}$ (M represents a metal cation, while O refers to an oxygen anion). The compounds stoichiometry plays a great role on the effect of structural stability under irradiation in certain fluorite derivative structures. Isometric pyrochlore structure, $A_2B_2O_7$, is a promising host phase for the immobilization of actinides [6–11]. For instance, in the binary system $Gd_2Ti_{2-x}Zr_xO_7$, the resistance to ion beam irradiation-induced amorphization increases dramatically with increasing Zr content, because of the cation and anion substructures disordered gradually as Zr content increases [2,12–14]. These studies illustrate that the irradiation tolerance of pyrochlore structure ($A_2B_2O_7$) is not only affected by the radius ratio $r_A/r_B$ and type of A–O and B–O bonds, but also affected by the level of initial cation structural disordering [11,15].

Another family of radiation tolerant fluorite-derivative oxides $A_4B_3O_{12}$ known as δ-phase possesses rhombohedral symmetry (space group $R\bar{3}$) of the fluorite structure with ordered oxygen vacancies along the ⟨1 1 1⟩ direction. One-seventh of all cation sites are in a 6-fold coordination by oxygen on a site of trigonal symmetry. The remaining six-sevenths of the cations are surrounded by seven oxygen atoms. The δ-phase materials have been shown to exhibit astonishing amorphization resistance characteristics due

* Corresponding author.
*E-mail address:* liyuhong@lzu.edu.cn (Y.H. Li).

http://dx.doi.org/10.1016/j.nimb.2015.04.011
0168-583X/

to their natural tendency to accommodate lattice disorder. In previous studies, no "4:3:12" δ-phase compounds have exhibited irradiation-induced amorphization. However, δ-phase compounds do undergo an order-to-disorder (O-D) phase transformation from an ordered rhombohedral to a disordered cubic fluorite structure. In particular, δ-$Sc_4Zr_3O_{12}$ does undergo O-D transformation and no amorphization has been observed even at very high radiation dose (~70 dpa) [16].

In this study, we choose to examine the ion induced radiation response of another δ-phase compound. The compound we chose to examine is $Sc_4Hf_3O_{12}$ which possesses a different cation arrangement from δ-$Sc_4Zr_3O_{12}$ which has been the focus of many studies [16–20]. In $Sc_4Hf_3O_{12}$ the cations are partially ordered compared to the complete disordering in $Sc_4Zr_3O_{12}$ [21]. The purpose of the study presented here is to investigate radiation damage effects and ion species spectrum effect in δ-$Sc_4Hf_3O_{12}$ by irradiating this compound with light and heavy ions. In another aspect, we will elucidate how cation ordering level affects the radiation damage behavior in δ-phase compounds. Finally, we discuss the effect of irradiation-induced cation antisite and anion oxygen Frenkel-pair defects on the O-D transformation in δ-$Sc_4Hf_3O_{12}$.

## 2. Experimental procedure

Polycrystalline pellets of the δ-$Sc_4Hf_3O_{12}$ were synthesized from high purity $Sc_2O_3$ (Alfa Aesar, 99.99%) and $HfO_2$ (Aldrich Chemical company, 99.99%) powders by conventional ceramic processing procedures. The pellets were then cut and polished to a mirror finish using 0.25 μm diamond suspension. X-ray diffraction measurements revealed that the pristine oxide ceramics possess a rhombohedral symmetry, δ-phase $Sc_4Hf_3O_{12}$ structure. The measured density of the $Sc_4Hf_3O_{12}$ sample was 6.40 g/cm$^3$, close to ~93% of the theoretical value ($\rho_{theoretical}$ = 6.90 g/cm$^3$).

Samples of δ-$Sc_4Hf_3O_{12}$ were irradiated with 400 keV $Ne^{2+}$ and 600 keV $Kr^{3+}$ ions at cryogenic temperature (~77 K) in the Ion Beam Materials Laboratory at Los Alamos National Laboratory, using a 200 kV Danfysik High Current Research Ion Implanter. The 400 keV $Ne^{2+}$ ions were implanted at normal incidence using ion fluences ranging from $1 \times 10^{14}$ to $1 \times 10^{15}$ ions/cm$^2$ and the average ion flux was maintained at ~$1 \times 10^{12}$ Ne/cm$^2$/s during the implantations, while the heavy ion irradiation was performed with 600 keV $Kr^{3+}$ ions to fluences ranging from $5 \times 10^{14}$ to $5 \times 10^{15}$ ions/cm$^2$, with an ion flux of ~$1 \times 10^{12}$ Kr/cm$^2$/s. The 6 MeV $Xe^{26+}$ ion irradiation was carried out at room temperature (~300 K) to ion fluences ranging from $2 \times 10^{13}$ to $1 \times 10^{15}$ ions/cm$^2$ with an ion flux of ~$1 \times 10^{11}$ Xe/cm$^2$/s on 320 kV platform for multi-discipline research with highly charged ions at the Institute of Modern Physics, Chinese Academy of Sciences (CAS). The projected ranges of the above ion species into δ-$Sc_4Hf_3O_{12}$ were estimated using the Monte Carlo program SRIM [22] and the results are listed in Table 1. The electronic to nuclear stopping power ratio (ENSP) and displacements per atom (dpa) were also calculated using SRIM [22]. The threshold displacement energies of Sc, Hf and O were assumed to be 40 eV in the simulation (because neither the theoretical or experimental values are known). The plots showing the ENSP simulation results are shown in Fig. 1a and it shows that electronic stopping plays a greater role in the total stopping power for 400 keV Ne and 6 MeV Xe ions, while the nuclear stopping plays a greater role for 600 keV Kr ions. Fig. 1b shows the displacement damage for Ne, Kr and Xe ions at the fluence of $1 \times 10^{15}$ ions/cm$^2$. The maximum peak displacement damage is approximately 0.33 dpa at the depth of 0.39 μm for $Ne^{2+}$ ions, ~2.2 dpa at the depth of 0.12 μm for $Kr^{3+}$ ions and ~4.86 dpa at the depth of 1.05 μm for $Xe^{26+}$ ions.

The pristine and ion irradiated samples were characterized using both grazing incidence X-ray diffraction (GIXRD) and transmission electron microscopy (TEM). GIXRD measurements were made using a Bruker AXS D8 Advanced X-ray Diffractometer, with Cu-Kα radiation operating in $\theta$–$2\theta$ geometry. The X-ray incidence angle for these measurements was chosen as $\gamma = 0.25°$, which is slightly smaller than the calculated critical angle $\alpha_c = 0.3°$ [23,24]. Under these conditions, X-rays are scattered from the surface of these samples to a depth of less than 100 nm [24,25]. This is much shallower than the 400 keV Ne, 600 keV Kr and 6 MeV Xe ion ranges shown in Fig. 1b. Therefore, we believe that the GIXRD measurements examined only the irradiated section, in the vicinity of

**Table 1**
SRIM projected range and longitudinal straggling, and measured O-D transformation threshold dose of three ion irradiation conditions used.

| Ion beam type | 400 keV $Ne^{++}$ | 600 keV $Kr^{3+}$ | 6000 keV $Xe^{26+}$ |
|---|---|---|---|
| Projected range (μm) | 0.65 | 0.32 | 1.50 |
| Straggling (μm) | 0.13 | 0.07 | 0.30 |
| Threshold dose (dpa) | 0.33 | 2.20 | >4.86 |

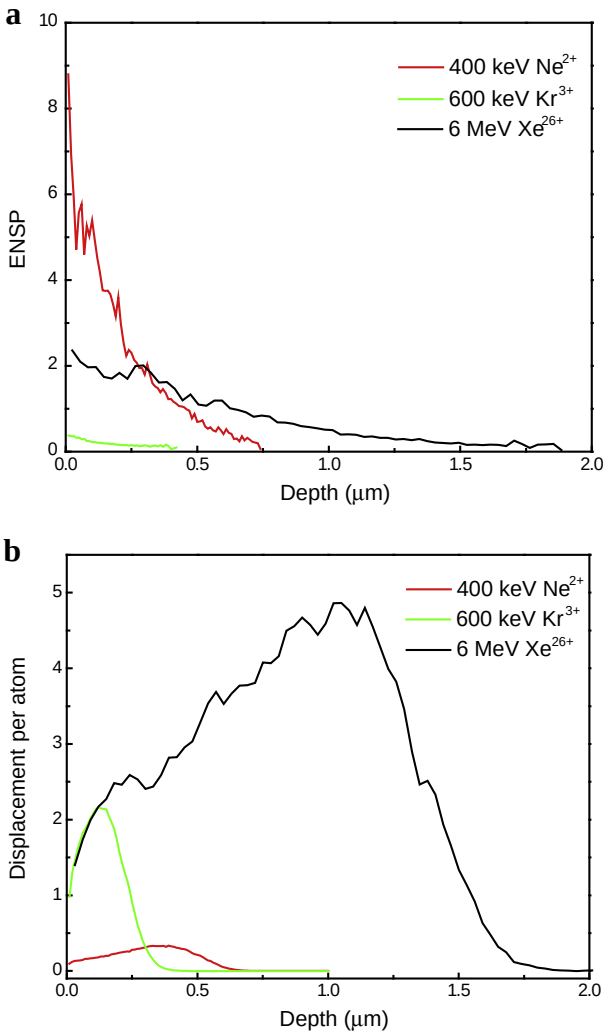


**Fig. 1.** (a) Electronic to nuclear stopping power ratio (ENSP) as a function of penetration depth calculated from data obtained from SRIM simulations for 400 keV Ne, 600 keV Kr and 6 MeV Xe into $Sc_4Hf_3O_{12}$. (b) SRIM calculation results plotting displacement per atom as a function of penetration depth for 400 keV Ne, 600 keV Kr and 6 MeV Xe ion irradiations into $Sc_4Hf_3O_{12}$ at a fluence of $1 \times 10^{15}$ ions/cm$^2$. (We used the density of 6.90 g/cm$^3$ and the threshold displacement energy of 40 eV for Sc, Hf and O).

the sample surface. The $\theta$–$2\theta$ scans were performed using a step size of 0.02° and a dwell time of 4 s. The scan range was 15–65°. Transmission electron microscopy (TEM) was performed on irradiated samples prepared in cross-sectional geometry. The TEM specimens were prepared by first mechanically polishing the sample to a thickness of less than 10 μm with diamond lapping films and then thinning the thickness down to electron transparency using 4 keV $Ar^+$ ion milling. Irradiation induced microstructures were examined using a FEI Tecnai F30 electron microscope operating with an accelerating voltage of 300 kV.

## 3. Results

Fig. 2a shows GIXRD patterns obtained from δ-$Sc_4Hf_3O_{12}$ samples before and after 400 keV $Ne^{2+}$ ion irradiation to fluences of $1 \times 10^{14}$ to $1 \times 10^{15}$ ions/cm$^2$. The patterns reveal that the superlattice reflections labeled with "δ" (referred to the δ-phase rhombohedral structure) diminish with increasing the ion fluence and completely disappear at the highest fluence of $1 \times 10^{15}$ ions/cm$^2$, which is equivalent to a peak ballistic damage dose of ~0.33 dpa. On the contrary, the four major diffraction peaks (at ~31°, 36°, 52°, and 61°), which are associated with the "parent" fluorite structure labeled with "F", are unaltered after the irradiation. The loss of the δ-phase reflections with increasing ion irradiation fluence implies that $Sc_4Hf_3O_{12}$ gradually underwent an O-D transformation, from an ordered δ-phase rhombohedral structure to a disordered cubic fluorite structure. Fig. 2b shows a cross-sectional TEM bright field (BF) image and selected area electron diffraction (SAED) patterns obtained from $Sc_4Hf_3O_{12}$ irradiated to a fluence of $1 \times 10^{15}$ Ne/cm$^2$ (~0.33 dpa). The Ne ion produced damage region shown in the bright field image was measured to be ~650 nm, in good agreement with the SRIM simulations results. The SAED patterns obtained from the substrate layer and the irradiated layer, indicating that structural changes are induced by the ion irradiation. The substrate SAED pattern can be indexed as a δ-phase rhombohedral structure along the beam direction of $\vec{B} = [1\bar{4}\bar{7}]_\delta$, while the SAED pattern obtained from the irradiation layer is indexed as a cubic fluorite structure along the beam direction of $\vec{B} = [1\bar{1}0]_F$. In summary, both the GIXRD patterns and TEM diffraction patterns show that Ne irradiated $Sc_4Hf_3O_{12}$ compound undergoes an O-D phase transformation at a fairly low peak displacement damage dose of ~0.33 dpa using 400 keV Ne ions.

Fig. 3a shows GIXRD patterns obtained from pristine $Sc_4Hf_3O_{12}$ and $Sc_4Hf_3O_{12}$ irradiated with 600 keV $Kr^{3+}$ ions to fluences ranging from $5 \times 10^{14}$ to $5 \times 10^{15}$ ions/cm$^2$. These ion fluences correspond to peak displacement damages of ~1.1 to ~11 dpa. The superlattice reflections (labeled with δ) diminish by a fluence of $5 \times 10^{14}$ ions/cm$^2$ and disappear completely at the fluence of $1 \times 10^{15}$ ions/cm$^2$ (~2.2 dpa). At the same time, the four principal diffractions corresponding to the "parent" fluorite structure (labeled "F" in the Fig. 3a) remain relatively unchanged after irradiation up to the highest fluence of $5 \times 10^{15}$ ions/cm$^2$ (~11 dpa). The observed changes in the GIXRD patterns imply that $Kr^{3+}$ ion irradiation induced a phase transformation in $Sc_4Hf_3O_{12}$, from an ordered δ-phase structure to a disordered fluorite structure. As a confirmation to GIXRD observations, TEM characterization was also performed on the 600 keV $Kr^{3+}$ ion irradiated sample. Fig. 3b shows a cross-sectional TEM bright-field image and SAED patterns obtained from the sample irradiated to a fluence of $1 \times 10^{15}$ ions/cm$^2$ (~2.2 dpa). The Kr damage region, labeled as the irradiated layer in Fig. 3b, is approximately 320 nm thick which agrees with the SRIM projected range of 600 keV Kr ions shown in Fig. 1b. The SAED patterns (right) with arrows indicating the areas from where they were collected reveal that there is an O-D phase transformation produced by the Kr ion irradiation. The top SAED pattern is indexed as a cubic fluorite structure with beam direction of $\vec{B} = [112]$; the bottom SAED pattern corresponding to the unirradiated region is indexed as an ordered rhombohedral δ-phase with beam direction of $\vec{B} = [211]$.

Fig. 4a shows GIXRD patterns obtained from pristine $Sc_4Hf_3O_{12}$ and $Sc_4Hf_3O_{12}$ irradiated with 6 MeV $Xe^{26+}$ ions to fluences of $2 \times 10^{13}$ to $1 \times 10^{15}$ ions/cm$^2$. The superlattice reflections (labeled with δ) diminish with increasing ion fluence, and almost disappear at highest fluence of $1 \times 10^{15}$ ions/cm$^2$ (~4.86 dpa). It implies that the complete O-D transformation should have occurred if a slightly higher fluence than $1 \times 10^{15}$ ions/cm$^2$ were used in the experiment. Fig. 4b shows the BF TEM image and SAED patterns of $Sc_4Hf_3O_{12}$ irradiated by Xe ions to a fluence of $1 \times 10^{15}$ ions/cm$^2$. The thickness of damage layer in BF TEM image is ~1.5 μm consistent with the SRIM calculation. The SAED pattern obtained from the irradiation region possesses two sets of diffraction patterns. The strong reflections are consistent with a cubic fluorite structure with beam direction $\vec{B} = [112]_F$, while the weaker reflections are equivalent to those in the pristine δ-phase patterns ($\vec{B} = [211]_\delta$). Combined GIXRD and TEM results, a partial structural transformation has occurred in $Sc_4Hf_3O_{12}$ irradiated by 6 MeV Xe ions to a fluence of $1 \times 10^{15}$ ions/cm$^2$ (~4.86 dpa).

## 4. Discussion

Based on GIXRD and TEM results for Ne, Kr and Xe ion irradiations on the δ-phase $Sc_4Hf_3O_{12}$, similar radiation response was observed: no evidence for a crystal-to-amorphous transformation was seen in any of these irradiations, while a phase transformation from an ordered δ-phase rhombohedral structure to a disordered fluorite cubic structure was observed under both electronic and nuclear stopping dominant irradiation environments. A complete O-D phase transformation was observed under both Ne and Kr ion irradiations, while a partial O-D phase transformation appeared under the Xe ion irradiation. In order to understand the process of the O-D phase transformation in δ-$Sc_4Hf_3O_{12}$, we will propose a possible mechanism in terms of a layered atom stacking model for the material [26]. The δ-phase rhombohedral structure can be described using a hexagonal unit cell which stacks three M layers and six O layers along the *c* axis. The stacking sequence of δ-$Sc_4Hf_3O_{12}$ is MOVOMOVOM, where M represents a layer consisting only of cations and O represents a pure layer of oxygen anions, V represents a completely vacant layer. The atoms in the M and O layers are actually rumpled out-of-plane by less than 4% of the *c* lattice parameter along *c* axis [26]. Fig. 5 illustrates the atomic arrangement discussed above showing the cation M (blue spheres) and anion O (red spheres) layers in δ-$Sc_4Hf_3O_{12}$. While the M layer (metal cations) consists of full dense triangular atom nets (Fig. 5a), the O layer consists of oxygen anions in triangular atom nets but also contains ordered empty sites within each layer (Fig. 5b). Each O layer is analogous to a 6/7 dense (partially-dense) $3^4{\cdot}6$ Archimedean tiling compared to a 7/7 (fully-dense) triangular atom net M layer. Several previous studies concluded that the order-to-disorder phase transformation of δ-phase compound is attributed to the effects of anion oxygen Frenkel-pair defects [16,19,27–29]. It is reasonable to assume that the order-to-disorder phase transformation in δ-$Sc_4Hf_3O_{12}$ is also due to anion oxygen Frenkel-pair defect. The process of O Frenkel pair formation during the irradiation is shown in Fig. 5c and d. O atoms on the proper lattice sites jump into the vacant sites in the O layer until the vacancies in the anion sublattices are randomly distributed. Therefore, if the ordered anion vacancies became random upon ion irradiation, the δ-phase rhombohedral distortion would be

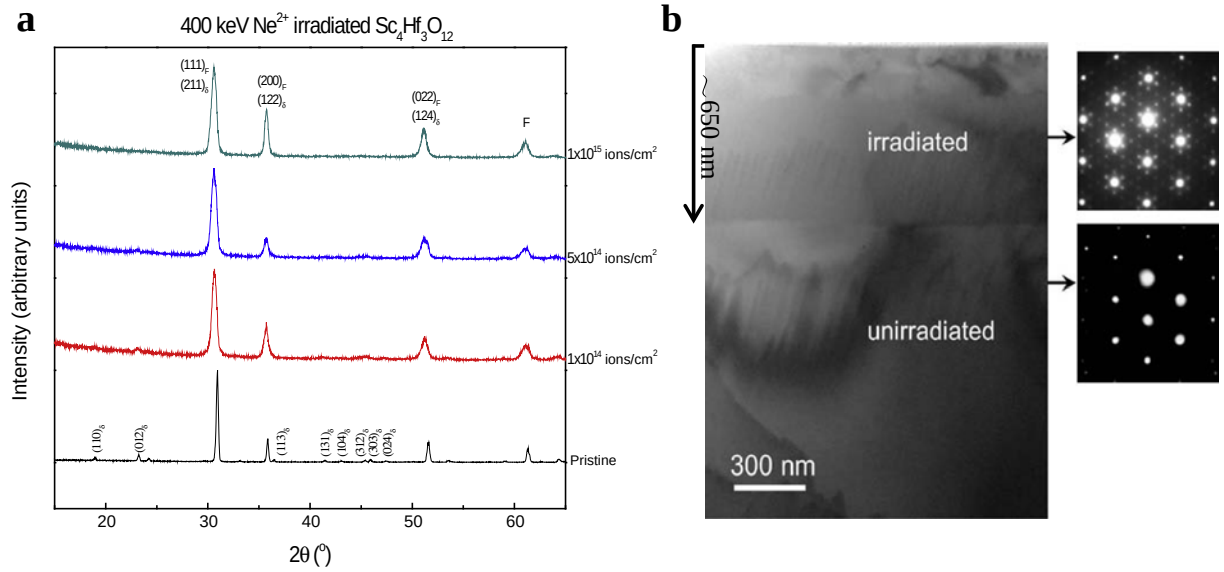


**Fig. 2.** (a) GIXRD patterns obtained from pristine and irradiated $Sc_4Hf_3O_{12}$ samples with 400 keV $Ne^{2+}$ ions to fluences of $1 \times 10^{14}$ to $1 \times 10^{15}$ ions/cm$^2$. Peaks labeled "δ" are the superlattice reflections associated with the ordered rhombohedral δ-phase, while the peaks labeled "F" are from the parent fluorite structure. (b) Cross-sectional bright-field TEM image with corresponding SAED patterns obtained from irradiated $Sc_4Hf_3O_{12}$ samples with 400 keV $Ne^{2+}$ ions to a fluence of $1 \times 10^{15}$ ions/cm$^2$ (~0.33 dpa).

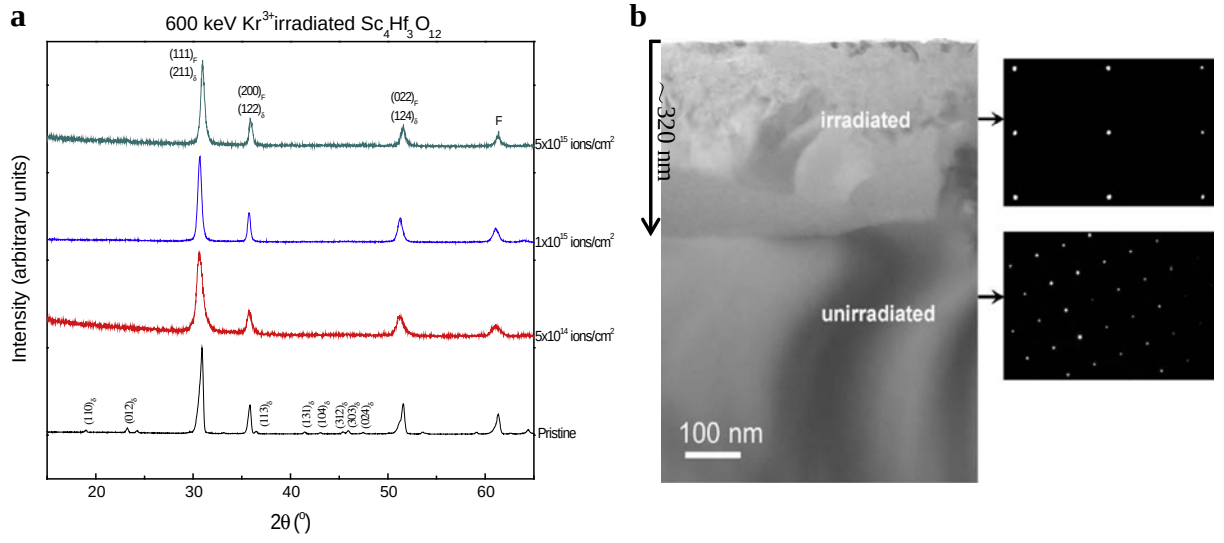


**Fig. 3.** (a) GIXRD patterns obtained from pristine and irradiated $Sc_4Hf_3O_{12}$ samples with 600 keV $Kr^{3+}$ ions to fluences of $5 \times 10^{14}$ to $5 \times 10^{15}$ ions/cm$^2$. (b) Cross-sectional bright-field TEM image with corresponding SAED patterns obtained from irradiated $Sc_4Hf_3O_{12}$ samples with 600 keV $Kr^{3+}$ ions to a fluence of $1 \times 10^{15}$ ions/cm$^2$ (~2.2 dpa).

relaxed to cubic which means the material had undergone an order-to-disorder transformation.

In the above discussions, we make the assumption that the two metal cations in δ-phase structures are randomly arranged in the M layers. This assumption may not be always true. In fact, depending on specific elemental compositions, the cations in M-layers in δ-phase structures could possess partial ordering [21]. For example, the cations in δ-$Sc_4Hf_3O_{12}$ are partially ordered in the M layers, while the cation arrangement in δ-$Sc_4Zr_3O_{12}$ is completely random (or fully disordered). Zhang et al. reported that δ-$Sc_4Zr_3O_{12}$ undergoes a full O-D transformation at a dose of ~2 dpa ($5 \times 10^{15}$ ions/cm$^2$) for Ne ions and a dose of ~23 dpa ($1 \times 10^{16}$ ions/cm$^2$) for Kr ions [19]. Such threshold doses for O-D phase transformation in δ-$Sc_4Zr_3O_{12}$ are significantly higher than that in δ-phase $Sc_4Hf_3O_{12}$ observed here. It suggests that the level of cation ordering in the pristine structure may have an important effect on the radiation-resistance of a given δ-phase compound based on its cation chemistry. Therefore, due to the partial ordering of the cations in pristine δ-$Sc_4Hf_3O_{12}$, it is reasonable to consider the effect of the cation antisite-pair defects produced during ion irradiation as a possible factor leading to the O-D transformation for this material. Based on X-ray diffraction theory structure factors [30], the amount of cation disordering can be calculated from the δ-phase superlattice reflections intensity ratio of {012} over {211} miller indices. The {012} indices is from one of the rhombohedral δ-phase superlattice reflections and the {211} indices is from one of the "parent" fluorite reflections. The result for δ-$Sc_4Hf_3O_{12}$ is shown in Fig. 6, indicating that the peak intensity ratio of {012} over {211} gradually decreases with increasing the amount of Sc and Hf cation antisite pairs ($Sc_{Hf}$ + $Hf_{Sc}$). Fig. 6 suggests that the cation antisite defects do play a role for the phase transformation in δ-$Sc_4Hf_3O_{12}$ during the ion irradiation.

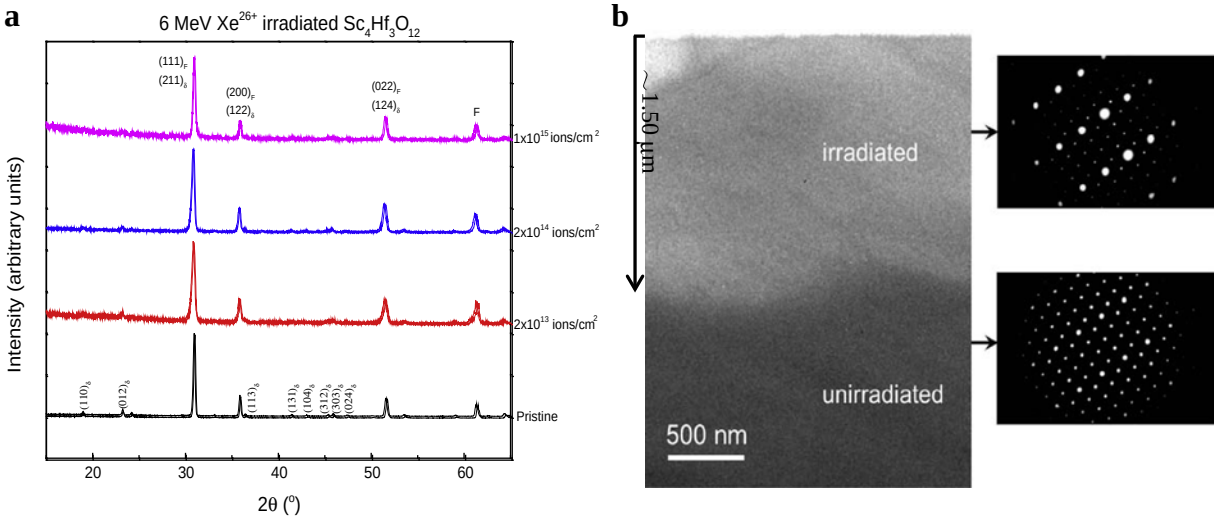


**Fig. 4.** (a) GIXRD patterns obtained from pristine and irradiated $Sc_4Hf_3O_{12}$ samples with 6 MeV $Xe^{26+}$ ions to fluences of $2 \times 10^{13}$ to $1 \times 10^{15}$ ions/cm$^2$. (b) Cross-sectional bright-field TEM image with corresponding SAED patterns obtained from irradiated $Sc_4Hf_3O_{12}$ samples with 6 MeV $Xe^{26+}$ ions to a fluence of $1 \times 10^{15}$ ions/cm$^2$ (~4.86 dpa).

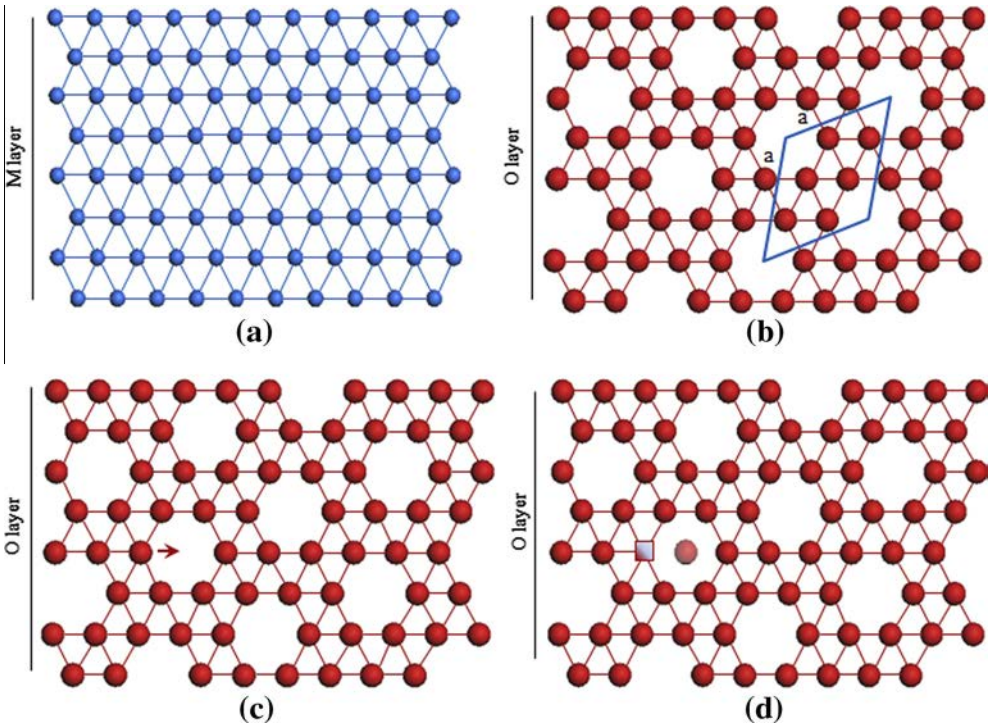


**Fig. 5.** Schematic diagram showing the stacking of the metal and oxygen layers along the *c*-axis for the hexagonal description of δ-$Sc_4Hf_3O_{12}$, along with a sample illustration of a Frenkel diffusion mechanism for this compound. (a) Cation (M) layer atom arrangement based on full dense triangular atom nets. (b) Oxygen atoms arranged in a $3^4{\cdot}6$ Archimedean tiling pattern. The atoms in real δ-$Sc_4Hf_3O_{12}$ are slightly rumpled away from the perfect triangular atom net in (a) and the $3^4{\cdot}6$ Archimedean tiling pattern in (b). (c) An O layer, with the jump direction for an atom near the vacancy. (d) The atom arrangement following the jump of the atom in (c) into the vacancy in the tiling pattern. The interstitial O atom is light in red. The vacancy left behind is shown as a red-shaded square. Diagrams (c) and (d) schematically represent radiation-induced (or in general) anion disorder. (For interpretation of the references to color in this figure legend, the reader is referred to the web version of this article.)

Considering the remarkable difference of the phase transformation dose between δ-$Sc_4Hf_3O_{12}$ and δ-$Sc_4Zr_3O_{12}$, we speculate that both the cation antisite defects and the oxygen Frenkel-pair defects have contributed to the irradiation-induced O-D transformation in δ-$Sc_4Hf_3O_{12}$. The above results imply that a δ-phase structure with completely disordered cations is more resistant to ion irradiation than with partially ordered cations.

Finally, a strong "ion species spectrum effect", which was first discovered in metals [31,32] and was also confirmed in studies on δ-$Sc_4Zr_3O_{12}$ ceramic compound [19], is also clearly demonstrated in δ-$Sc_4Hf_3O_{12}$. The threshold O-D transformation doses for three ion irradiations used in this study are listed in Table 1. The different transformation threshold dose observed between heavy and light ions are likely related to the Frenkel pair defects recombination and survival efficiency. The displacement cascades produced by heavy ions are denser compared to those produced by light ions. In other words, Frenkel pair defects by heavy ions have a higher annihilating probability, such as interstitial/vacancy

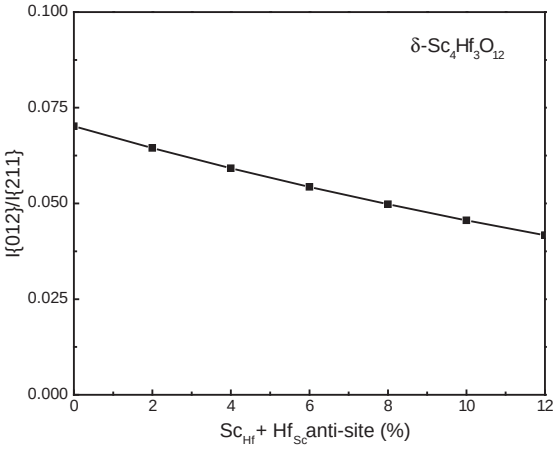


**Fig. 6.** Calculated intensity radio of $I\{0\,1\,2\}/I\{2\,1\,1\}$ miler indices in δ-$Sc_4Hf_3O_{12}$ as a function of the relative ratio of cation antisite pair defects.

recombination, than those produced by light ions. As a result, defect survivability is reduced under heavy ion irradiation condition. Therefore, heavy ions require a larger irradiation fluence to induce O-D transformation in δ-$Sc_4Hf_3O_{12}$ than the light ions. Another reasonable interpretation concerning to "ion species spectrum effect" could be the energy transfer efficiency during the ion–atom collisions as defined by $\Lambda = 4M_1M_2/(M_1 + M_2)^2$, where $M_1$ and $M_2$ are the atomic masses of the projectile and target element [33]. Considering anion Frenkel pair production, Ne ions have the highest energy transfer efficiency to O atoms (0.987), followed by Kr ions (0.538), and finally Xe ions (0.450). In other words, light ions are more efficient than heavy ions in transferring their kinetic energy to O anions and thus changing O vacancy arrangement from order to disorder in O sublattices. In summary, we believe that both cascade density and kinetic energy transfer efficiency have contributed to the observed "ion species spectrum effect" in δ-$Sc_4Hf_3O_{12}$ compound.

## 5. Conclusions

The irradiation damage response in δ-$Sc_4Hf_3O_{12}$ by heavy and light ion irradiations have been systematically investigated using grazing incidence X-ray diffraction (GIXRD) and transmission electron microscopy (TEM). A crystal structure transformation from an ordered rhombohedral to a disordered fluorite structure occurred under both light and heavy ion irradiations. However, the transformation dose for the heavy ions is higher than the dose required transforming the material when irradiating with the light ions. This effect that was observed during this investigation on δ-$Sc_4Hf_3O_{12}$ is consistent with previous studies, in which both metals and ceramics also succumb to an ion spectrum effect. It is noted that the partial cation ordering existing in δ-$Sc_4Hf_3O_{12}$ prior-irradiation may be a factor in making it more susceptible to ion-induced order to disorder transformations as compared to other δ-phase materials that possess fully disordered cation sublattices. Our results lead to the fact that both anion Frenkel defects and cation antisite defects contribute to irradiation-induced O-D phase transformation in the δ-$Sc_4Hf_3O_{12}$.

## Acknowledgments

This work was sponsored by the National Natural Science Foundation of China (11475076 and 11175076). The work was also sponsored by the U.S. Department of Energy (DOE), Office of Basic Energy Science. Partial support to J. Wen was provided by China Scholarship Council, a nonprofit organization affiliated with the Ministry of Education of China. We acknowledge the support by the operational staff at the 320 kV platform for multi-discipline research with highly charged ions at the Institute of Modern Physics, CAS.

## References

[1] W.J. Weber, R.C. Ewing, C.R.A. Catlow, T.D. De La Rubia, L.W. Hobbs, C. Kinoshita, H.J. Matzke, A.T. Motta, M. Nastasi, E.K.H. Salje, E.R. Vance, S.J. Zinkle, J. Mater. Res. 13 (1998) 1434–1484.
[2] S.X. Wang, B.D. Begg, L.M. Wang, R.C. Ewing, W.J. Weber, K.V. Govidan Kutty, J. Mater. Res. 14 (1999) 4470–4473.
[3] K.E. Sickafus, L. Minervini, R.W. Grimes, J.A. Valdez, M. Ishimaru, F. Li, K.J. McClellan, T. Hartmann, Science 289 (2000) 748–751.
[4] R.C. Ewing, W.J. Weber, J. Lian, J. Appl. Phys. 95 (2004) 5949–5971.
[5] K.E. Sickafus, R.W. Grimes, J.A. Valdez, A. Cleave, M. Tang, M. Ishimaru, S.M. Corish, C.R. Stanek, B.P. Uberuaga, Nat. Mater. 6 (2007) 217–223.
[6] W.J. Weber, R.C. Ewing, Science 289 (2000) 2051.
[7] Y.H. Li, B.P. Uberuaga, C. Jiang, S. Choudhury, J.A. Valdez, M.K. Patel, J.H. Won, Y.Q. Wang, M. Tang, D.J. Safarik, D.D. Byler, K.J. McClellan, I.O. Usov, T. Hartmann, G. Baldinozzi, K.E. Sickafus, Phys. Rev. Lett. 108 (2012) 195504.
[8] M. Lang, J. Lian, J.M. Zhang, F.X. Zhang, W.J. Weber, C. Trautmann, R.C. Ewing, Phys. Rev. B 79 (2009) 224105.
[9] L. Minervini, R.W. Grimes, K.E. Sickafus, J. Am. Ceram. Soc. 83 (2000) 1873–1878.
[10] Y.H. Li, J. Wen, Y.Q. Wang, Z.G. Wang, M. Tang, J.A. Valdez, K.E. Sickafus, Nucl. Instrum. Meth. B 287 (2012) 130–134.
[11] J. Lian, J. Chen, L.M. Wang, R.C. Ewing, J.M. Farmer, L.A. Boatner, K.B. Helean, Phys. Rev. B 68 (2003) 134107.
[12] S.X. Wang, L.M. Wang, R.C. Ewing, K.V.G. Kutty, MRS Proc. 540 (1999) 355.
[13] B.D. Begg, N.J. Hess, D.E. McCready, S. Thevuthasan, W.J. Weber, J. Nucl. Mater. 289 (2001) 188–193.
[14] N.J. Hess, B.D. Begg, S.D. Conradson, D.E. McCready, P.L. Gassman, W.J. Weber, J. Phys. Chem. B 106 (2002) 4663–4677.
[15] J.M. Zhang, J. Lian, F.X. Zhang, J.W. Wang, A.F. Fuentes, R.C. Ewing, J. Phys. Chem. C 114 (2010) (1815) 11810–11811.
[16] J.A. Valdez, M. Tang, K.E. Sickafus, Nucl. Instrum. Meth. B 250 (2006) 148–154.
[17] M. Ishimaru, Y. Hirotsu, M. Tang, J.A. Valdez, K.E. Sickafus, J. Appl. Phys. 102 (2007) 063532.
[18] K.E. Sickafus, M. Ishimaru, Y. Hirotsu, I.O. Usov, J.A. Valdez, P. Hosemann, A.L. Johnson, T.T. Thao, Nucl. Instrum. Meth. B 266 (2008) 2892–2897.
[19] J. Zhang, Y.Q. Wang, M. Tang, J.H. Won, J.A. Valdez, K.E. Sickafus, J. Mater. Res. 25 (2010) 248–254.
[20] J. Zhang, Y.Q. Wang, J.A. Valdez, M. Tang, K.E. Sickafus, J. Nucl. Mater. 419 (2011) 386–391.
[21] H.J. Rossell, H.G. Scott, Le Journal de Physique Colloques 38 (1977). C7-28-C27-31.
[22] J.F. Ziegler, J.P. Biersack, U. Littmark, The Stopping and Range of Ions in Matter (SRIM), Available from: <http://www.srim.org>.
[23] A. Guinier, X-ray Diffraction in Crystals, Imperfect Crystals and Amorphous Bodies, Dover Publications Inc, New York, 1994.
[24] G. Lim, W. Parrish, C. Ortiz, M. Bellotto, M. Hart, J. Mater. Res. 2 (1987) 471.
[25] D. Simeone, J.L. Bechade, D. Gosset, A. Chevarier, P. Daniel, H. Pilliaire, G. Baldinozzi, J. Nucl. Mater. 281 (2000) 171–181.
[26] K.E. Sickafus, R.W. Grimes, S.M. Corish, A.R. Cleave, M. tang, C.R. Stanek, B.P. Uberuaga, J.A. Valdez, Layered Atom Arrangements in Complex Materials, Los Alamos Series Report No, LA-14205, 2006.
[27] J. Zhang, Y.Q. Wang, M. Tang, J.A. Valdez, K.E. Sickafus, Nucl. Instrum. Meth. B 268 (2010) 3018–3022.
[28] J. Wen, C. Gao, Y.H. Li, Y.Q. Wang, L.M. Zhang, B.T. Hu, L.J. Chen, X. Su, Nucl. Instrum. Meth. B 310 (2012) 1–5.
[29] L.J. Chen, X. Su, J. Wen, D.Y. Yang, Y.H. Li, B.T. Hu, J. Appl. Phys. 114 (2013) 083714.
[30] B.D. Cullity, Elements of X-ray Diffraction, Add-wesley Publishing company Inc, Reading, MA, 1956.
[31] R.S. Averback, R. Benedek, K.L. Merkle, Phys. Rev. B 18 (1978) 4156.
[32] R.S. Averback, J. Nucl. Mater. 216 (1994) 49.
[33] P. Sigmund, Theory of Displacement Damage, Ion Ranges and Sputtering, Rev. Roum. Phys. 17 (1972) 823.